

ORIGINAL ARTICLE

Effect of Horizontal and Vertical Intraoral Scan Bodies on the Trueness of Complete-Arch Digital Implant Impressions: A Comparative In Vitro Study With Six Implants

Luís Azevedo^{1,2}  | Andrea Laureti^{1,3} | Tiago Marques^{2,4} | João Pitta¹  | Vincent Fehmer¹ | Alessandro Pozzi^{5,6,7,8} | Irena Sailer¹ 

¹Division of Fixed Prosthodontics and Biomaterials, University Clinics for Dental Medicine, University of Geneva, Geneva, Switzerland | ²Center for Interdisciplinary Research in Health, The Catholic University of Portugal (UCP), Viseu, Portugal | ³Department of Chemical Science and Technologies, University of Rome Tor Vergata, Rome, Italy | ⁴Faculty of Dental Medicine, The Catholic University of Portugal (UCP), Viseu, Portugal | ⁵Department of Clinical Science and Translational Medicine, University of Rome Tor Vergata, Rome, Italy | ⁶Goldstein Center for Esthetic and Implant Dentistry, Department of Restorative Science, The Dental College of Georgia at Augusta University, Augusta, Georgia, USA | ⁷Department of Periodontics and Oral Medicine, University of Michigan School of Dentistry, University of Michigan, Ann Harbor, Michigan, USA | ⁸Department of Restorative Dentistry and Biomaterials Sciences, Harvard School of Dental Medicine, Boston, Massachusetts, USA

Correspondence: Luís Azevedo (luís.pereiraazevedo@unige.ch)

Received: 23 October 2024 | **Revised:** 8 May 2025 | **Accepted:** 3 June 2025

Keywords: complete arch | digital impression | horizontal scanbodies | intraoral scanner

ABSTRACT

Objective: To evaluate the interaction between intraoral scan body (ISB) type, operator, and intraoral scanner (IOS) selection on the trueness of complete-arch digital implant impressions. This study also compared horizontal ISBs (H-ISBs) and vertical ISBs (V-ISBs) across four IOS devices.

Material and Methods: Digital impressions of a definitive mandibular cast with six multi-unit analogs were made using four H-ISBs from different manufacturers (denoted as H-NB, H-NS, H-M6, and H-SF), with a V-ISB (V-EA) as the reference. Each ISB was scanned using a desktop scanner and by two operators who scanned each ISB system 10 times using four IOS devices i5D, PS, T3, T4, generating 400 digital impressions. Deviations were measured using root-mean-square (RMS) error ($\alpha = 0.05$).

Results: All independent variables (operator, IOS, ISB) significantly affected trueness ($p < 0.05$). V-EA with i5D had the lowest trueness (78 [27] μm), while H-NS on PS showed the highest (12 [3] μm). H-M6 maintained high trueness across IOS devices. PS was the most stable IOS, while T4 showed the most variability.

Conclusions: Complete-arch digital impressions are influenced by ISBs, IOSs, and operators. H-ISBs demonstrated better trueness and consistency across IOSs and operators.

1 | Introduction

Success of implant-supported complete-arch prostheses relies on achieving a passive fit to prevent biological and technical failures such as screw loosening and fractures (Jemt 2017; Pan

et al. 2021; Toia et al. 2019). Achieving this precise fit requires exceptional clinical and laboratory accuracy, starting with an accurate recording of implant positions using either digital or conventional impression techniques (Papaspnyridakos, Vazouras, et al. 2020; Wulfman et al. 2020; Cheng et al. 2024).

Conventional implant impression techniques, such as the open-tray implant impression method with splinted impression copings, are accurate but time-consuming and require laborious manual procedures (Joda and Brägger 2016; Joda et al. 2017). While conventional methods remain the standard with reported high accuracy (Gómez-Polo et al. 2022; Blanco-Plard et al. 2023; Tohme et al. 2023; Jasim et al. 2024; Ali et al. 2024), they are prone to errors due to material limitations (Pozzi et al. 2013).

With computer-aided design computer-aid manufacture (CAD/CAM) technology, a completely digital workflow is possible for fabricating implant-supported prostheses (Brandt et al. 2015). The first step involves recording the exact implant position with an intraoral scanner (IOS) and an intraoral scan body (ISB). IOSs, consisting of a handheld camera, computer, and software, capture and analyze reflected light to generate 3D images. IOS technology is favored for its improved patient comfort and clinical efficiency (Joda and Brägger 2016; Joda et al. 2017).

However, IOS accuracy can be affected by operator and patient-related factors, especially in edentulous arches (Revilla-León et al. 2023a, 2023b). IOS devices use image stitching, enhanced by anatomical reference points, to align consecutive images (Retana et al. 2023). While suitable for single crowns and short-span prostheses, scanning a complete edentulous arch is challenging due to the lack of landmarks and the difficulty in distinguishing multiple ISBs (Gómez-Polo et al. 2022; Patzelt et al. 2014).

To improve accuracy, the use of horizontally positioned ISBs (H-ISBs) of varying heights and lengths helps eliminate gaps and inconsistencies between ISBs. Unlike traditional vertically placed ISBs (V-ISBs), the horizontal design allows for a more streamlined, single-pass scanning process, reducing image overlap and stitching errors as the clinician moves along the arch (Giglio et al. 2024; Klein et al. 2023). This concept aligns with the approach of splinting ISBs (Cheng et al. 2024; Ali et al. 2024; Retana et al. 2023; Cappare et al. 2019; Mizumoto et al. 2020; Kanjanasavitree et al. 2022; Pozzi et al. 2022; Azevedo et al. 2024a), as seen in several studies, as well as the addition of soft tissue artificial landmarks (Mizumoto et al. 2020;

Kanjanasavitree et al. 2022; Azevedo et al. 2024a; Chochlidakis et al. 2020; Papaspyridakos, Chochlidakis, et al. 2020; Rutkūnas et al. 2023).

Although H-ISBs offer potential advantages, no studies, to the best of the authors' knowledge, have directly compared their trueness to V-ISBs across various IOS systems. This study seeks to address this gap by assessing the trueness of H-ISBs in complete-arch digital implant impressions. This study aimed to evaluate how the interaction between ISB type (horizontal vs. vertical) and IOS selection influences the trueness of complete-arch digital implant impressions. Additionally, the study compared the trueness of different ISB designs across various IOSs to determine which combinations yielded the highest accuracy. The null hypothesis was that neither ISB type nor IOS selection, individually or in combination, would affect trueness.

2 | Material and Methods

A definitive cast of an edentulous mandible with a soft tissue replica was fabricated and used as the reference cast. Six parallel dental implant analogs (multi-unit analogs, Nobel Biocare, Switzerland) in the first molar, first premolar, and lateral incisors positions located 3 mm below the model's surface were placed. Ethics approval was not required for this study, as it was an in vitro investigation using a dental cast with no involvement of human participants or patient data.

For the experimental groups, four H-ISBs from various manufacturers were selected and denoted as H-NB (Nobel Biocare Multi-unit Polo, Nobel Biocare, Switzerland), H-NS (Nexus Scan Gauges, Nexus iOS, Australia), H-M6 (M6 Dental Multi-unit abutment, MY Digital Implant, China) and H-SF (SmartFlags, Apollo, Poland). In addition, a vertical ISB (Elos Accurate, Nobel Biocare, Switzerland), referred to as V-EA, was chosen as the gold standard reference. Figure 1 represents all the ISBs evaluated in the study. The H-ISBs varied in both material and design: H-NB, H-NS, and H-M6 were made entirely of titanium, with H-NB and H-M6 featuring a two-piece configuration where a horizontal component was screwed into the main body,

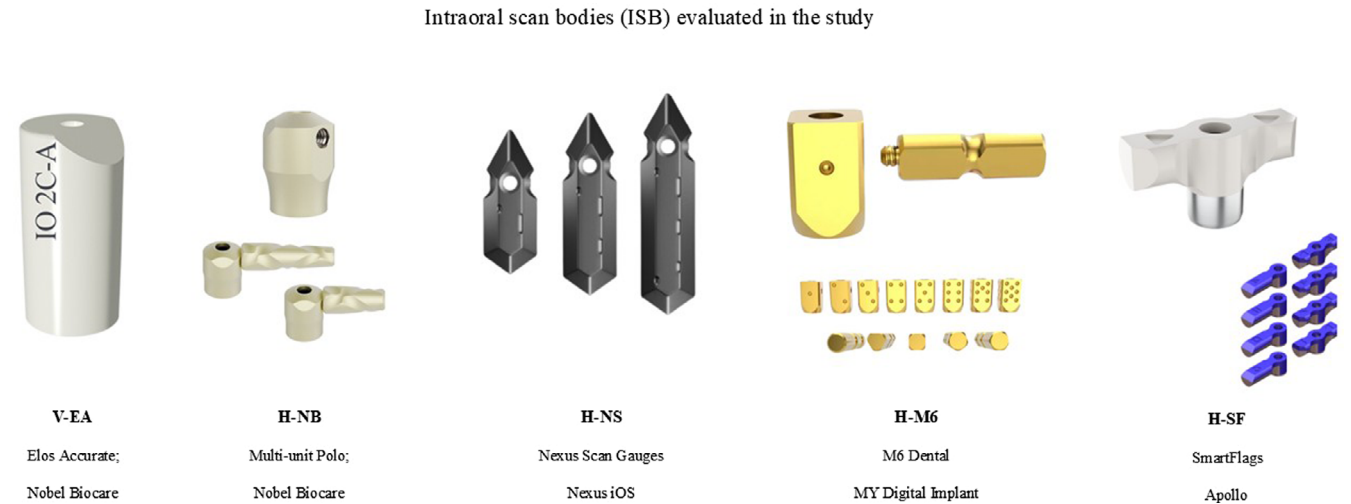


FIGURE 1 | Intraoral scan bodies (ISBs) of various designs (vertical and horizontal) from different manufacturers included in the study.

whereas H-NS had a single-piece construction. H-SF incorporated a medical-grade polymer (PEEK) with an anti-reflective surface to enhance the scan, while its titanium base ensured a secure implant connection. In contrast, the V-ISB (V-EA) was a single-piece ISB made entirely of PEEK. All the H-ISBs and the V-ISB were tightened to 10 Ncm by using an automatic torque control unit (Endo-mate TC2, NSK, Japan) and were not moved between registrations to avoid positional errors. Each ISB was visually inspected to ensure its integrity and adherence to manufacturer specifications.

A desktop scanner (IScan4D LS3i, Imetric 4D, Switzerland) with an accuracy of $\pm 5\mu\text{m}$ for implant scans, according to the manufacturer, was used to scan the reference cast to obtain the reference digital cast (RDC) (Doukantzis et al. 2021; Marchand et al. 2022; Lee et al. 2020). The digitized dental casts were saved as a standard tessellation language file (STL) to serve as the RDC. The desktop scanner was calibrated according to the manufacturer's guidelines. For each ISB type, a reference dental cast was obtained and scanned to establish an accurate baseline for comparison.

Four different IOSs were used with each group: TRIOS 3 (T3) and TRIOS 4 (T4) (3Shape, Denmark), iTero Element 5D (i5D) (Align Technology, USA), and Primescan (PS) (Dentsply Sirona, USA). The scanning strategy applied for all the digital scans was the zig-zag technique, as used in previous studies (Pattamavilai and Ongthiemsak 2022; Tasaka et al. 2019), starting from the most distal ISB of the fourth quadrant. Two operators (L.A. and A.L.) with more than 5 years of experience using IOSs, after three training sessions of 20 min with each IOS, performed all digital scans by using the most recent acquisition software program available for each IOS. Scanning parameters, including resolution (high-definition mode), depth, and angulation, were kept consistent for all scans.

Ten consecutive digital scans ($n=10$) of the RDC were made with the 4 IOSs, in a temperature and humidity-controlled

environment (Revilla-León et al. 2021). The groups were scanned in a random order generated by a spreadsheet (Excel; Microsoft Corp). The STL files from both the IOSs and the desktop scanner were imported into CAD software (exocad DentalCAD 3.1 Rijeka, exocad GmbH, Germany) to align the digital scans with the CAD library's ISB, ensuring the same multi-unit abutment analog for all files to facilitate 3D evaluation and comparison (Figure 2). All alignments with the corresponding library's ISB were performed by the same person (L.A.), who had experience working with CAD software. After importing all multi-unit STL files, they were imported into metrology software (Geomagic Control X 2022.1; 3D Systems Inc., USA) for comparison and analysis of deviation (trueness) by superimposing the digital analogs (digital multi-unit abutments). The RDC was used as the reference. Subsequently, the surfaces of the STL files were aligned for optimal superimposition by using the "Align Between Measured Data" and "Best-Fit Alignment" functions. The overall deviation was assessed by using the "3D Compare" function, which generated a color map of the superimposed digital casts to quantitatively analyze the 3-dimensional (3D) changes. The color map ranged from $+0.3\text{mm}$ to -0.3mm , with a tolerance range of $\pm 0.02\text{mm}$. The mean RMS error indicated the deviation value (trueness). The RMS is a mathematical parameter that measures the size of a dataset. The RMS values are calculated by taking the square root of the average of the squared differences between the corresponding points on the two digital multi-unit abutments. Figure 3 illustrates the digital analysis workflow.

The main dependent outcome was the trueness of each technique tested, measured in microns (μm). Trueness assessed how close the digitized test object (ISBs) was to the true dimensions of the RDC.

Descriptive statistics, including median, interquartile range (IQR), minimum, and maximum values, were calculated. Initially, a random intercept mixed model was fit to account for

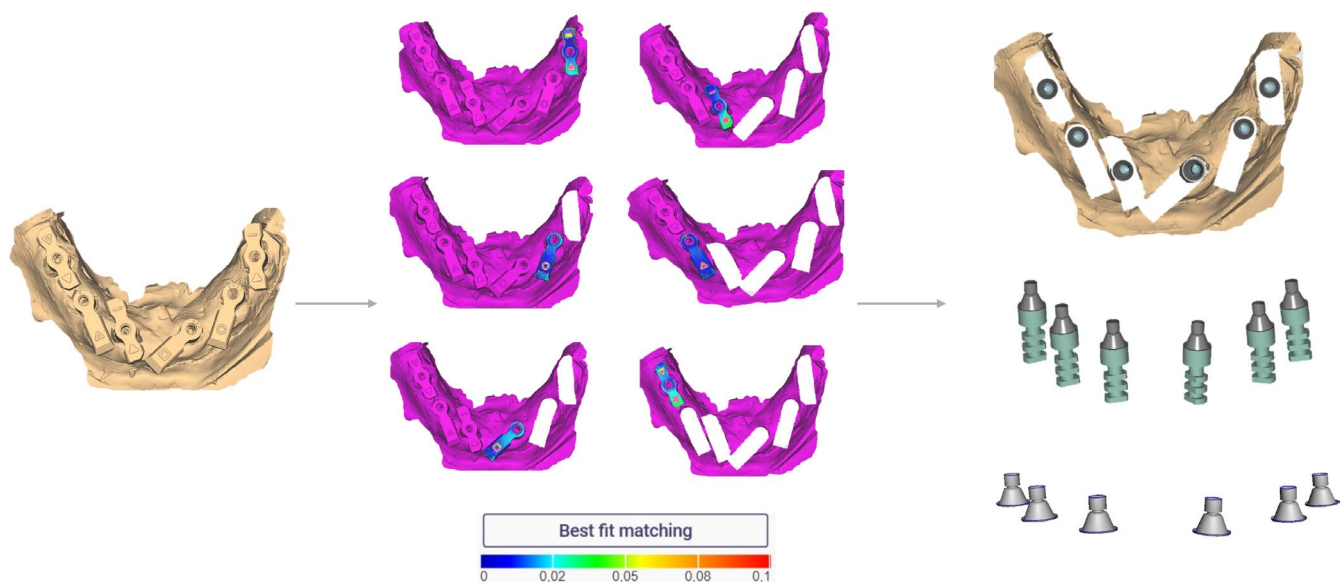


FIGURE 2 | Digital workflow for aligning STL files from intraoral and desktop scanners with the CAD library's scan body (ISB) using exocad software (exocad DentalCAD, exocad GmbH), standardizing the multi-unit abutment for 3D evaluation and comparison.

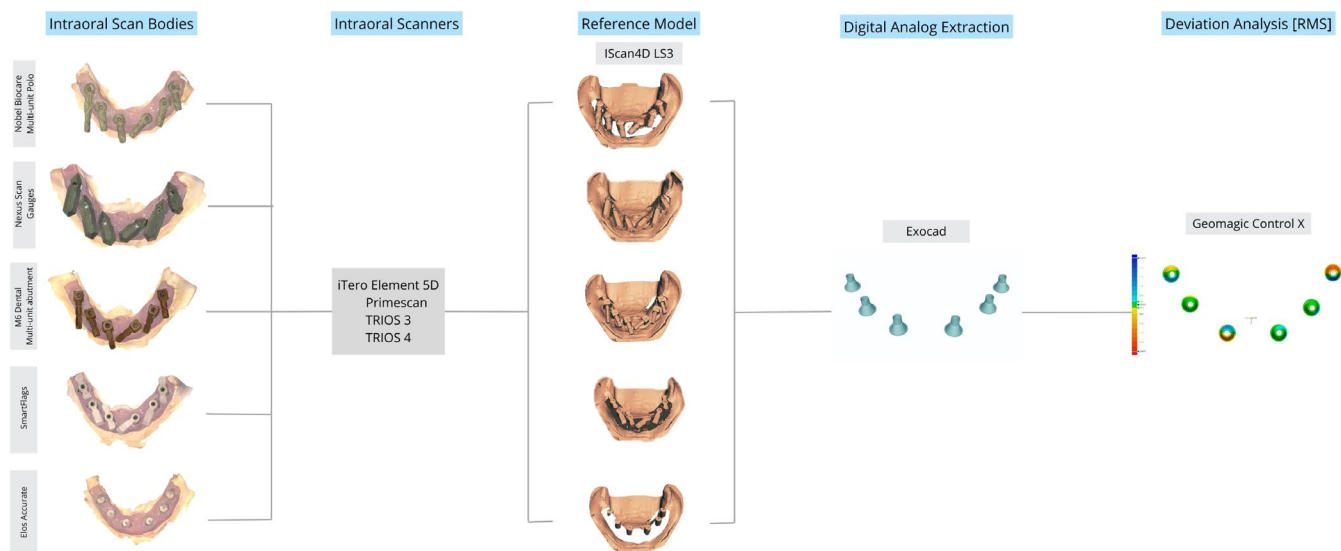


FIGURE 3 | Summary of the 3D digital analysis for the superimposition of scans according to the “Best-fit Alignment” method in Geomagic Control X.

the correlated nature of the data. However, the likelihood ratio test compared to the uncorrelated model was not significant ($p=0.78$), and the covariance for the mixed model was close to zero, suggesting that the repeated measurements were not correlated. Therefore, the simpler linear model was chosen. The linear model used RMS as the dependent variable, with operator, IOS, ISB, and their interactions as the independent variables. Wald tests were conducted for the main effects and interactions. A Tukey test was used to evaluate the differences between the groups. Trueness was defined as the amount of average 3D deviation between the corresponding ISBs in the test scan and the RDC. The level of significance was set at $p<0.05$. All analyses were conducted using Stata 18.0 (StataCorp, USA).

3 | Results

Descriptive statistics for RMS values across ISBs and IOSs combinations are presented in Table 1. The histogram indicated a distribution close to normal for the outcome variable. Although the Shapiro–Wilk test yielded $p<0.05$, given the large sample size ($n=400$), the histogram was considered a more reliable indicator of normality.

Overall, the V-ISB consistently demonstrated lower trueness (higher RMS values), particularly with the iTero Element 5D, where V-ISB had the highest RMS value (77 [28] μm). In contrast, H-ISBs generally exhibited higher trueness (lower RMS values), with Primescan achieving the best performance for H-NS (12 [4] μm), which represented the highest trueness in the study. TRIOS 3 showed consistently high trueness across all ISBs, while TRIOS 4 had more variability, with H-NB showing the lowest trueness (39 [13] μm).

When comparing ISBs without considering IOS, V-EA had significantly lower trueness than all H-ISBs ($p<0.001$). Differences among H-ISBs were minimal, except for occasional variations with H-SF in comparison with H-M6 ($p=0.015$). For IOSs without considering ISBs, iTero Element 5D showed the lowest

trueness ($p<0.001$), while Primescan consistently had the highest trueness across conditions.

When comparing ISBs within the same IOS, the iTero Element 5D had the lowest trueness for V-EA ($p<0.001$), with significant differences between the two operators. In contrast, H-ISBs demonstrated much lower variation in trueness regardless of the operator. Comparing IOSs within the same ISB revealed that Primescan consistently outperformed other IOSs, especially with H-NB and H-NS, showing the highest trueness across multiple ISBs ($p<0.001$).

Regression analysis showed that operator, ISB, and IOS all significantly influenced RMS values ($p<0.05$), with significant interaction effects ($p<0.001$) (Table 2). However, the most pronounced operator-dependent differences were found exclusively with the V-ISB when used with iTero Element 5D. In contrast, H-ISB showed stable, low RMS values across different IOSs and operators.

Figures 4, 5, and 6 illustrate these findings. Figure 4 presents boxplots of RMS values grouped by ISB, IOS, and operator, illustrating the distribution of RMS values. This figure provides a comparative analysis of operator consistency and performance across various scanbody-scanner combinations, using RMS values as an indicator of scanning trueness. Figures 5 and 6 demonstrate the predicted RMS values with 95% confidence intervals, highlighting the significant inconsistencies for V-ISB with iTero Element 5D between operators, while other ISB-IOS combinations showed overlapping confidence intervals (no significant differences), suggesting a minimal operator effect.

Figures 4, 5, and 6 illustrate these findings. Figure 4 presents boxplots of RMS values grouped by ISB, IOS, and operator, illustrating the distribution of RMS values. This figure provides a comparative analysis of operator consistency and performance across various scanbody-scanner combinations, using RMS values as an indicator of scanning trueness. Figures 5 and 6 demonstrate the predicted RMS values with 95% confidence intervals,

TABLE 1 | Median, interquartile range (IQR), minimum and maximum mean root-mean-square (RMS) values of different intraoral scan bodies (ISBs) for each intraoral scanner (IOS) (μm).

		iTero Element 5D		Primescan		TRIOS 3		TRIOS 4	
		Median (IQR)	Min-max	Median (IQR)	Min-max	Median (IQR)	Min-max	Median (IQR)	Min-max
Operator 1	V-EA	68 (12) ^{a;α}	54–80	25 (8) ^{a;β}	13–36	20 (6) ^{a;β,γ}	14–38	33 (11) ^a	25–47
	H-NB	22 (4) ^{b;α}	15–28	13 (3) ^{a,b;α,β}	11–19	21 (7) ^{a,b;α,β,γ}	18–32	36 (15) ^{a,b}	30–48
	H-NS	29 (3) ^{b,c;α}	19–32	14 (2) ^{a,b,c;β}	10–15	24 (3) ^{a,b,c;α,β,γ}	22–30	40 (11) ^{a,b,c;α,γ}	26–45
	H-M6	18 (17) ^{b,c,d;α}	12–52	26 (3) ^{a,d;α,β}	18–32	20 (5) ^{a,b,c,d;α,β,γ}	11–35	22 (9) ^{d;α,β,γ}	15–29
	H-SF	35 (5) ^{b,c,d;α}	24–40	12 (7) ^{a,b,c;β}	4–19	32 (10) ^{a,b,c,d;α,γ}	21–41	31 (7) ^{a,b,c,d;α,γ}	27–48
Operator 2	V-EA	95 (17) ^{a;α}	56–117	29 (9) ^{a;β}	11–39	22 (6) ^{a;β,γ}	20–35	36 (15) ^{a;β}	23–57
	H-NB	22 (5) ^{b;α}	17–27	17 (5) ^{a,b;α,β}	12–25	24 (6) ^{a,b;α,β,γ}	16–31	42 (11) ^{a,b}	31–49
	H-NS	32 (5) ^{b,c;α}	28–37	10 (2) ^{b,c;β}	10–12	21 (7) ^{a,b,c;α,β,γ}	18–30	33 (5) ^{a,b,c;α,γ}	29–37
	H-M6	30 (18) ^{b,c,d;α}	14–50	21 (5) ^{a,b,c,d;α,β}	12–34	21 (2) ^{a,b,c,d;α,β,γ}	20–28	24 (11) ^{c,d;α,β,γ}	15–43
	H-SF	31 (9) ^{b,c,d;α}	26–39	18 (6) ^{a,b,c,d;β}	12–31	22 (3) ^{a,b,c,d;α,β,γ}	19–24	34 (7) ^{a,b,c,d;α}	28–41

Note: Values sharing the same letter within a column (a, b, c and d) and within a row (α , β and γ), for each operator, are not statistically different at the 5% level. Tukey adjustment applied for multiple comparisons.

TABLE 2 | Contrasts for main effects and interaction terms (Wald tests).

	Degrees of freedom	F	p
Operator	1	5.66	0.020
ISB	4	94.86	<0.001
IOS	3	185.75	<0.001
Operator \times IOS interaction	3	7.71	<0.001
Operator \times ISB interaction	4	6.88	<0.001
IOS \times ISB interaction	12	62.41	<0.001
Operator \times IOS \times ISB interaction	12	4.88	<0.001

highlighting the significant inconsistencies for V-ISB with iTero Element 5D between operators, while other ISB-IOS combinations showed overlapping confidence intervals (no significant differences), suggesting a minimal operator effect.

4 | Discussion

The findings of the present study emphasize the significant influence of the operator, IOS, and ISB on the trueness of

complete-arch digital impressions. The results highlight that while all main effects and interactions between these factors were statistically significant, the most critical inconsistency was observed with the iTero Element 5D when used with the V-ISB. This suggests that the accuracy of complete-arch digital impressions is not only device-dependent but also highly affected by scan body design and individual operator technique, leading to the rejection of the null hypothesis.

Regarding the comparison of different ISBs with the same IOS, the study found that V-EA exhibited lower trueness with both the iTero Element 5D and Primescan. However, the most notable variability was observed with iTero and V-EA, particularly for Operator 2. The higher RMS values for this combination suggest a greater susceptibility to operator-related inconsistencies, possibly due to the design and material of the V-ISB. The PEEK material of V-ISB may be less compatible with the optical scanning technology of iTero, aligning with previous research indicating better performance with metal ISBs (Azevedo et al. 2024b).

From a design perspective, IOS systems primarily scan ISBs along the vertical axis (z -axis), initially capturing the narrow top portion before acquiring data from the curved sides. The reliance on an internal accelerometer for positional tracking introduces errors when excessive movement occurs, and increased lateral movement further exacerbates these errors, requiring additional image stitching (Giglio et al. 2024). H-ISBs help mitigate these challenges by providing a more stable horizontal scanning surface, reducing dependence on accelerometer adjustments and minimizing potential stitching errors

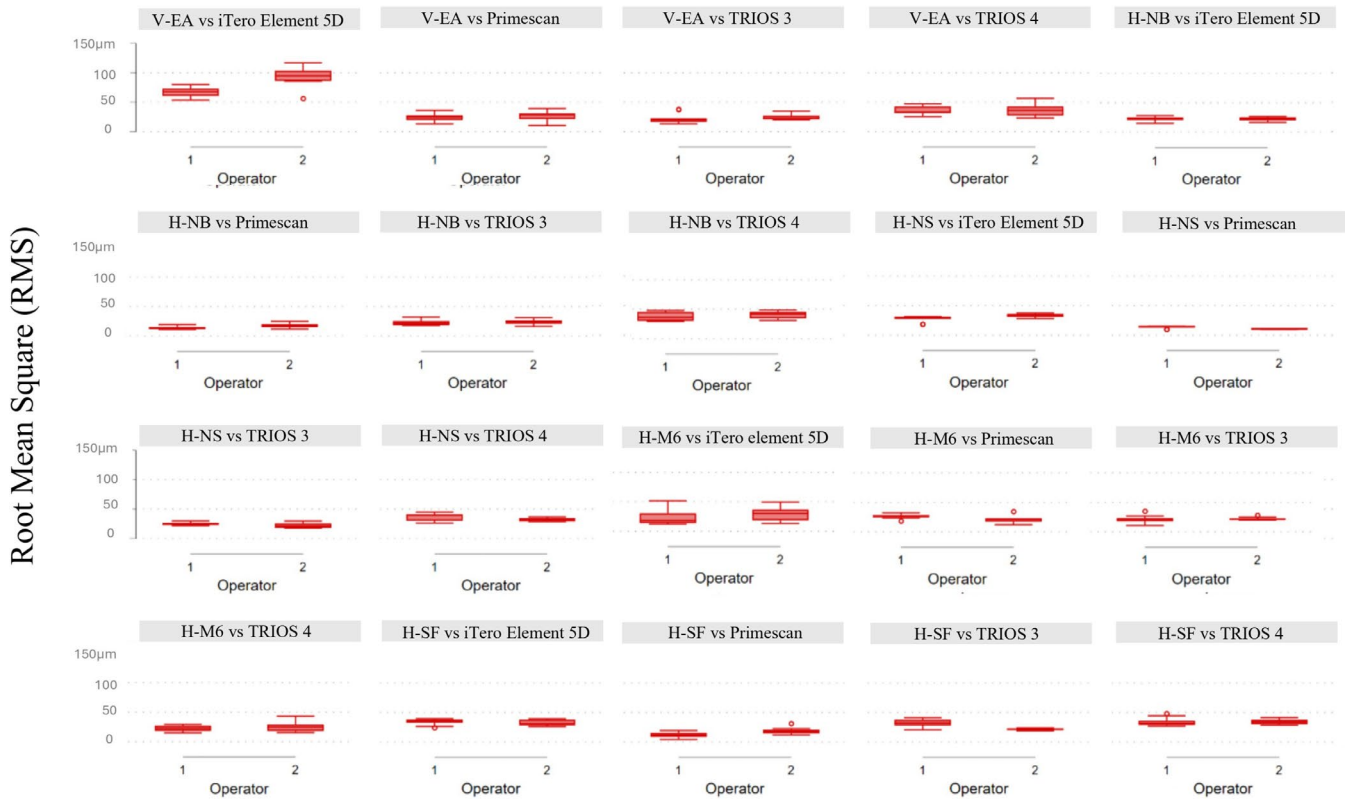


FIGURE 4 | Boxplots of the mean root-mean-square (RMS) by intraoral scanner (IOS), intraoral scan body (ISB) and operator.

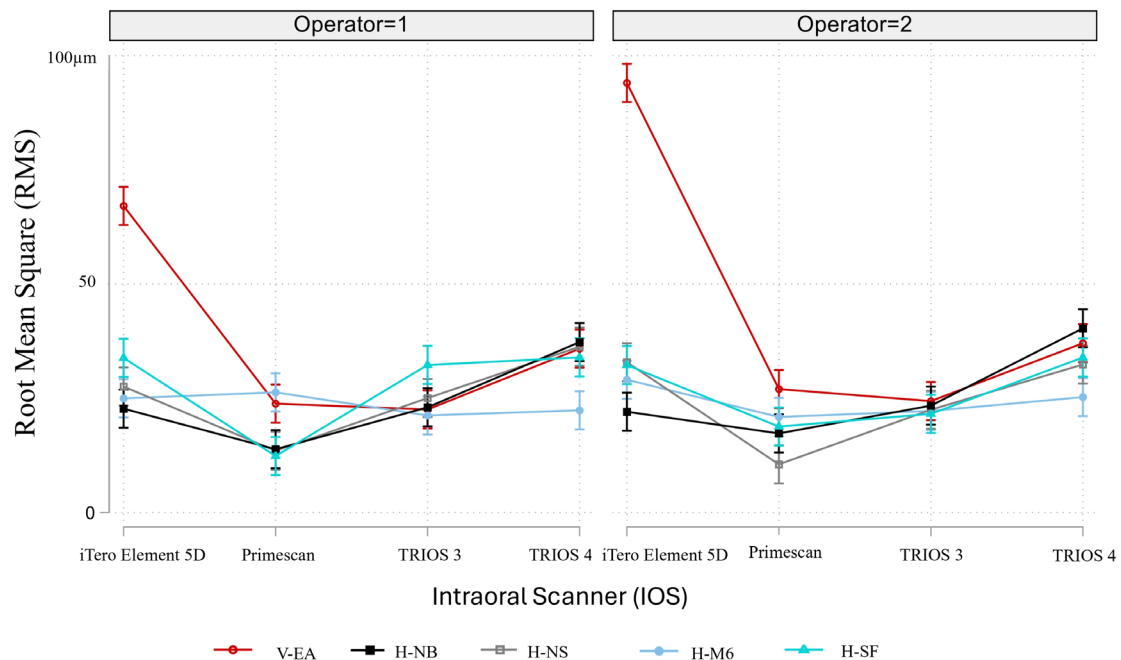


FIGURE 5 | Margin plots for mean root-mean-square (RMS) by operator, intraoral scanner (IOS) and intraoral scan body (ISB) with 95% confidence intervals. Non-overlapping confidence intervals indicate statistically significant differences between operators for specific ISB x IOS combinations.

(Giglio et al. 2024). This contributes to the observed consistency in trueness across operators when using H-ISBs, regardless of the IOS system.

To address these scanning limitations, H-ISBs were specifically designed to optimize digital impression accuracy. Their

horizontal orientation allows the IOS to capture more data points efficiently, reducing the need for excessive lateral movement and minimizing accelerometer-induced distortions. The multiple planes on H-ISBs provide a broader scanning surface, while their lower vertical profile enhances accessibility within the oral cavity. As a result, H-ISBs demonstrated superior trueness across

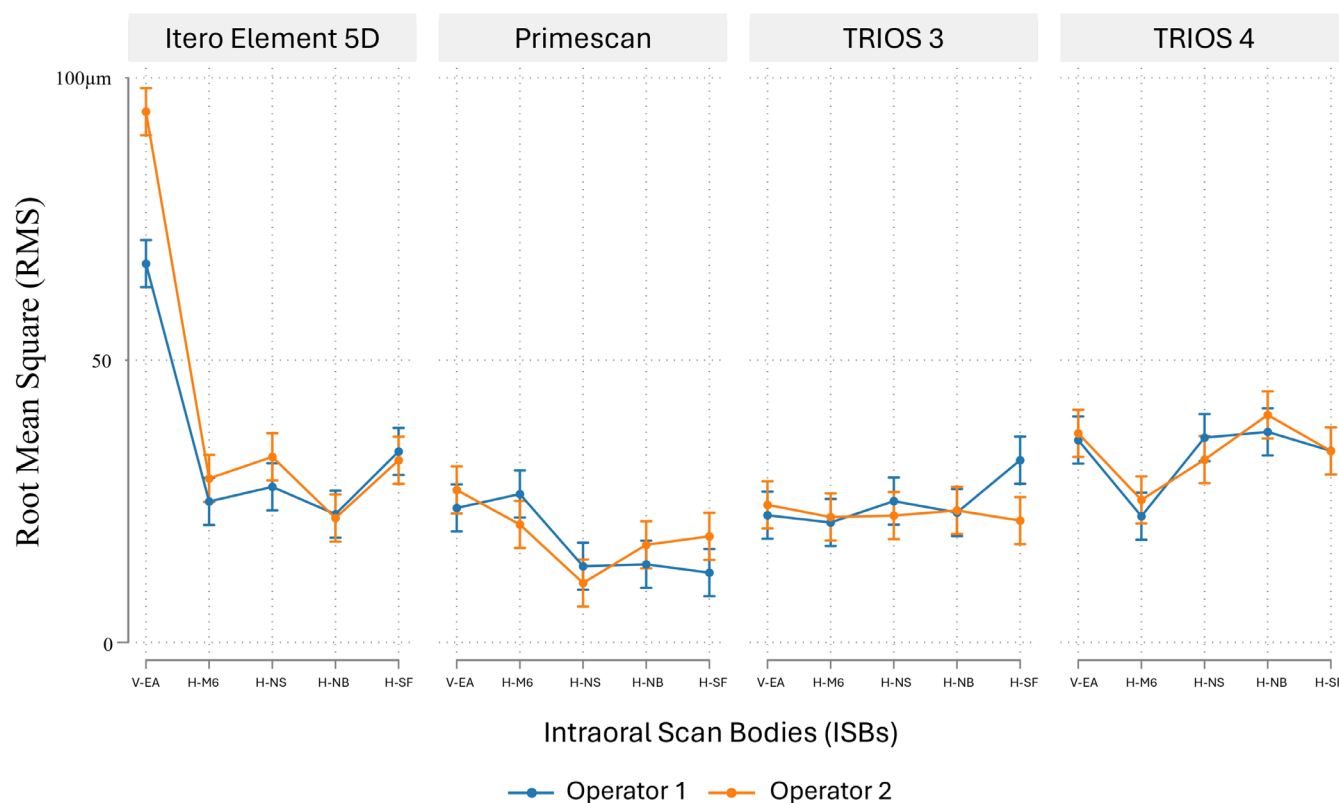


FIGURE 6 | Margin plots for mean root-mean-square (RMS) by operator, intraoral scanner (IOS), and intraoral scan body (ISB) with 95% confidence intervals. Non-overlapping confidence intervals indicate statistically significant differences between operators for specific ISB×IOS combinations.

multiple IOSs, particularly with the Primescan device. Factors such as reduced vertical height, improved scanner accessibility, and enhanced scanning surface area likely contribute to their improved performance. Future research should further explore how ISB design elements—such as geometry, height, retention system, and material—affect scanning accuracy.

Recent studies have focused on refining ISB designs to further enhance intraoral scanning accuracy, particularly for implant rehabilitation in edentulous patients (Zhang et al. 2024; Wu et al. 2024; Etxaniz et al. 2024; Canullo et al. 2024; Ashry et al. 2024; Wu et al. 2023; Huang et al. 2021; Huang et al. 2020). Huang et al. (Huang et al. 2020) investigated the accuracy of an original ISB design compared to two newly developed CAD/CAM ISBs—one with and one without an extensional structure. Their findings indicated that the extensional structure significantly improved scanning accuracy by providing additional horizontal reference points for the IOS (Huang et al. 2020). Other studies have explored auxiliary devices attached to ISBs or newly milled ISB designs incorporating horizontal structures to optimize digital impressions (Zhang et al. 2024; Wu et al. 2024; Etxaniz et al. 2024; Canullo et al. 2024; Ashry et al. 2024; Wu et al. 2023; Huang et al. 2021; Huang et al. 2020). These advancements highlight the ongoing evolution of ISB technology to improve trueness and consistency in implant scanning.

Primescan consistently achieved the highest trueness across all ISBs, particularly with H-NB, H-NS, and H-SF, showing the lowest RMS values. The low RMS values for Primescan, often under 20 μm, further demonstrate its superior accuracy, which aligns

with findings from previous studies (Azevedo et al. 2024a; Ashraf et al. 2023).

The results from TRIOS 3 and TRIOS 4 IOSs showed some discrepancies. TRIOS 4 exhibited higher RMS values (lower trueness) across all ISBs compared to TRIOS 3, echoing findings from other studies that reported lower trueness with Trios 4 (Azevedo et al. 2024a). This may be due to technological differences between the two scanner versions. Additionally, no significant difference in trueness was found between V-ISB and H-ISBs for both TRIOS scanners. Despite all the advantages of the horizontal design mentioned above, in this study, the six-implant model with closely spaced implants may have minimized the influence of H-ISBs on scan accuracy for the TRIOS systems. These findings align with the study by Denneulin et al. (2023) which assessed the effect of implant number and splinting on digital scanning accuracy in edentulous arches. Their results showed that splinting ISBs negatively affected accuracy in a six-implant model using the TRIOS 3 system, while splinting improved accuracy in a four-implant model. They concluded that both the number of implants and their distribution along the arch significantly influence scanning accuracy (Denneulin et al. 2023).

The effect of operator variability in digital impressions was only observed with V-EA using the iTero Element 5D device, where Operator 2 exhibited higher RMS values (lower trueness). While these differences were statistically significant, they were relatively small and not consistent across other ISBs and IOSs. This suggests that while the operator influences the accuracy of complete-arch digital impressions, the choice of ISB and IOS

may have a more pronounced effect on overall trueness. These findings highlight the importance of training and familiarity with specific IOSs and ISBs to optimize performance. Further studies with a larger operator sample are necessary to better understand the extent of operator-dependent variability.

The regression analysis further supports the importance of considering the interactions between IOS, ISB, and operator. The findings suggest that the best outcomes are achieved when these factors are evaluated together rather than individually. This is particularly important when selecting an IOS and ISB combination for complete-arch digital impressions, as the wrong pairing could introduce higher errors, as seen with the iTero Element 5D and V-ISB combination.

This study has several limitations. First, the in vitro design may not fully replicate clinical conditions, including patient movement, salivary contamination, and soft tissue dynamics, all of which can impact scan accuracy in a real-world setting. Additionally, the zigzag scanning protocol and variations in IOS technologies may have influenced the results, as different scanning strategies and technologies operate under distinct principles.

Furthermore, this study used an edentulous mandibular dental cast previously used in the authors' research (Azevedo et al. 2024a, 2024b), which may not fully account for anatomical differences between the maxilla and mandible. Future studies should incorporate both arches to comprehensively assess digital impression accuracy.

Regarding the assessment method, this study evaluated trueness using root-mean-square (RMS) analysis, which provides an overall 3D deviation measurement but does not account for individual implant positions. While this approach aligns with previous studies (Azevedo et al. 2024a, 2024b) and ensures comparability, future research should integrate vector-based analysis to examine deviations at specific implant sites, particularly in distal regions where accuracy may be lower. Vector-based analysis offers direct measurement of coordinate values (linear and angular deviations) and vectors, allowing for a more detailed evaluation of implant position accuracy. However, a best-fit alignment remains necessary to initially align the meshes and enable reliable comparisons, as discrepancies in orientation and positioning could introduce further errors. Additionally, multiple sources of error accumulate throughout the workflow, including CAD software alignment with the digital implant analog, scanner-associated errors, best-fit alignment errors, and fabrication inaccuracies, all of which may influence final deviation measurements. Future investigations should explore whether certain implant positions are more susceptible to deviations depending on the ISB and IOS combination.

Finally, while this study followed the recommended best practices for PEEK scan body use—including single-use application and controlled torque tightening (Gómez-Polo et al. 2023)—the potential for deformation remains a consideration. While the risk of distortion was minimized, existing literature suggests that metal ISBs generally provide superior accuracy compared to PEEK ISBs for complete-arch digital impressions (Azevedo et al. 2024b). However, at the time of the study, the official

scan body available in the market for Nobel Biocare multi-unit abutments was made of PEEK, leaving no alternative choice. Additionally, the absence of repeated measurements by multiple raters limited the ability to assess inter-rater reliability, highlighting the need for future studies to incorporate duplicate assessments for greater methodological rigor.

In future research, validating the clinical performance of H-ISBs in an intraoral setting will be crucial to understanding how in vivo factors affect digital impression accuracy. Additionally, the authors are conducting a follow-up in vitro study to analyze whether reducing the number of implants affects impression accuracy. Ultimately, the integration of new digital technologies should aim to enhance efficiency for both dentists and dental technicians without significantly increasing costs. The adoption of digital workflows must be evidence-based, with proper training and a streamlined learning curve to ensure smooth and effective implementation in clinical practice.

5 | Conclusion

This study demonstrated that the accuracy of complete-arch digital impressions is significantly influenced by the interaction between operator, IOS, and ISB type. The most notable inconsistency was observed with V-ISB when used with the iTero Element 5D, where operator-dependent variability was significant. In contrast, H-ISBs provided more consistent trueness across different operators and IOSs, particularly with the Primescan system.

Clinically, these findings suggest that H-ISBs may improve digital impression accuracy for complete-arch rehabilitations by minimizing operator-related inconsistencies. This consistency could potentially reduce the risk of prosthetic misfit. Given the multifactorial nature of digital impression accuracy, future studies should further investigate the role of ISB geometry, material properties, and scanning protocols across various clinical conditions. Additionally, incorporating vector-based analysis could provide a more detailed assessment of deviations at specific implant positions, complementing existing best-fit alignment techniques.

Author Contributions

Luís Azevedo: conceptualization, investigation, writing – original draft, data curation, methodology, software. **Andrea Laureti:** conceptualization, investigation, data curation, writing – original draft, methodology. **Tiago Marques:** writing – review and editing, validation, software, supervision. **João Pitta:** writing – review and editing, supervision, validation. **Vincent Fehmer:** writing – review and editing, project administration, resources, funding acquisition, supervision. **Alessandro Pozzi:** writing – review and editing, validation, supervision. **Irena Sailer:** writing – review and editing, supervision, validation, funding acquisition, project administration, resources.

Acknowledgments

The authors thank Prof Nikolaos Pandis for all the statistical support. The authors also thank all the companies for providing the intraoral scan bodies.

Conflicts of Interest

The authors declare no conflicts of interest.

Data Availability Statement

The data that support the findings of this study are available on request from the corresponding author. The data are not publicly available due to privacy or ethical restrictions.

References

- Ali, K., A. A. Alzaid, M. S. Suprono, A. Garbacea, R. Savignano, and M. T. Kattadiyil. 2024. "Evaluating the Effects of Splinting Implant Scan Bodies Intraorally on the Trueness of Complete Arch Digital Scans: A Clinical Study." *Journal of Prosthetic Dentistry* 132: 781.e1–781.e7.
- Ashraf, Y., A. Abo El Fadl, A. Hamdy, and K. Ebeid. 2023. "Effect of Different Intraoral Scanners and Scanbody Splinting on Accuracy of Scanning Implant-Supported Full Arch Fixed Prosthesis." *Journal of Esthetic and Restorative Dentistry* 35: 1257–1263.
- Ashry, A., A. M. Abdelhamid, S. Ezzelarab, and M. M. Khamis. 2024. "Effect of Using Scan Body Accessories and Inter-Implant Distances on the Accuracy of Complete Arch Implant Digital Impressions: An In Vitro Study." *Journal of Prosthodontics*. <https://doi.org/10.1111/jopr.13856>.
- Azevedo, L., T. Marques, D. Karasan, et al. 2024a. "Effect of Splinting Scan Bodies on the Trueness of Complete Arch Digital Implant Scans With 5 Different Intraoral Scanners." *Journal of Prosthetic Dentistry* 132: 204–210.
- Azevedo, L., T. Marques, D. Karasan, et al. 2024b. "Influence of Implant Scanbody Material and Intraoral Scanner on the Accuracy of Complete-Arch Digital Implant Impressions." *International Journal of Prosthodontics* 37: 575–582.
- Blanco-Plard, A., A. Hernandez, F. Pino, N. Vargas, S. Rivas-Tumanyan, and A. Elias. 2023. "3D Accuracy of a Conventional Method Versus Three Digital Scanning Strategies for Completely Edentulous Maxillary Implant Impressions." *International Journal of Oral & Maxillofacial Implants* 38: 1211–1219.
- Brandt, J., H. C. Lauer, T. Peter, and S. Brandt. 2015. "Digital Process for an Implant-Supported Fixed Dental Prosthesis: A Clinical Report." *Journal of Prosthetic Dentistry* 114: 469–473.
- Canullo, L., P. Pesce, V. C. A. Caponio, et al. 2024. "Effect of Auxiliary Geometric Devices on the Accuracy of Intraoral Scans in Full-Arch Implant-Supported Rehabilitations: An In Vitro Study." *Journal of Dentistry* 145: 104979.
- Cappare, P., G. Sannino, M. Minoli, P. Montemezzi, and F. Ferrini. 2019. "Conventional Versus Digital Impressions for Full Arch Screw-Retained Maxillary Rehabilitations: A Randomized Clinical Trial." *International Journal of Environmental Research and Public Health* 16: 829.
- Cheng, J., H. Zhang, H. Liu, J. Li, H. Wang, and X. Tao. 2024. "Accuracy of Edentulous Full-Arch Implant Impression: An In Vitro Comparison Between Conventional Impression, Intraoral Scan With and Without Splinting, and Photogrammetry." *Clinical Oral Implants Research* 35, no. 5: 560–572.
- Chochlidakis, K., P. Papaspyridakos, A. Tsigarida, et al. 2020. "Digital Versus Conventional Full-Arch Implant Impressions: A Prospective Study on 16 Edentulous Maxillae." *Journal of Prosthodontics* 29: 281–286.
- Denneulin, T., C. Rignon-Bret, G. Ravalec, L. Tapie, D. Bouter, and C. Wulfman. 2023. "Accuracy of Complete-Arch Implant Digital Scans: Effect of Scanning Protocol, Number of Implants, and Scan Body Splinting." *International Journal of Prosthodontics* 36: 219–227.
- Doukantzis, M., P. Mojon, A. Todorovic, et al. 2021. "Comparison of the Accuracy of Optical Impression Systems in Three Different Clinical Situations." *International Journal of Prosthodontics* 34: 511–517.
- Etxaniz, O., X. Amezuza, M. Jauregi, and E. Solaberrieta. 2024. "Improving the Accuracy of Complete Arch Implant Intraoral Digital Scans by Using Horizontal Scan Bodies With Occlusal Geometry: A Dental Technique." *Journal of Prosthetic Dentistry* 22: S0022-3913(24)00058-1.
- Giglio, G., A. Giglio, and D. Tarnow. 2024. "A Paradigm Shift Using Scan Bodies to Record the Position of a Complete Arch of Implants in a Digital Workflow." *International Journal of Periodontics & Restorative Dentistry* 44: 115–126.
- Gómez-Polo, M., M. B. Donmez, G. Çakmak, B. Yilmaz, and M. Revilla-León. 2023. "Influence of Implant Scan Body Design (Height, Diameter, Geometry, Material, and Retention System) on Intraoral Scanning Accuracy: A Systematic Review." *Journal of Prosthodontics* 32: 165–180.
- Gómez-Polo, M., A. Sallorenzo, R. Cascos, J. Ballesteros, A. B. Barmak, and M. Revilla-León. 2022. "Conventional and Digital Complete-Arch Implant Impression Techniques: An In Vitro Study Comparing Accuracy." *Journal of Prosthetic Dentistry* 132: 809–818.
- Huang, R., Y. Liu, B. Huang, C. Zhang, Z. Chen, and Z. Li. 2020. "Improved Scanning Accuracy With Newly Designed Scan Bodies: An In Vitro Study Comparing Digital Versus Conventional Impression Techniques for Complete-Arch Implant Rehabilitation." *Clinical Oral Implants Research* 31: 625–633.
- Huang, R., Y. Liu, B. Huang, F. Zhou, Z. Chen, and Z. Li. 2021. "Improved Accuracy of Digital Implant Impressions With Newly Designed Scan Bodies: An In Vivo Evaluation in Beagle Dogs." *BMC Oral Health* 21: 623.
- Jasim, A. G., M. G. Abo Elezz, G. Y. Altonbary, and M. A. Elsyad. 2024. "Accuracy of Digital and Conventional Implant-Level Impression Techniques for Maxillary Full-Arch Screw-Retained Prosthesis: A Crossover Randomized Trial." *Clinical Implant Dentistry and Related Research* 26: 714–723.
- Jemt, T. 2017. "A Retro-Pro prospective Effectiveness Study on 3448 Implant Operations at One Referral Clinic: A Multifactorial Analysis. Part I: Clinical Factors Associated to Early Implant Failures." *Clinical Implant Dentistry and Related Research* 19: 980–988.
- Joda, T., and U. Brägger. 2016. "Patient-Centered Outcomes Comparing Digital and Conventional Implant Impression Procedures: A Randomized Crossover Trial." *Clinical Oral Implants Research* 27: e185–e189.
- Joda, T., P. Lenherr, P. Dedem, I. Kovaltschuk, U. Bragger, and N. U. Zitzmann. 2017. "Time Efficiency, Difficulty, and Operator's Preference Comparing Digital and Conventional Implant Impressions: A Randomized Controlled Trial." *Clinical Oral Implants Research* 28: 1318–1323.
- Kanjanasavitree, P., P. Thammajaruk, and M. Guazzato. 2022. "Comparison of Different Artificial Landmarks and Scanning Patterns on the Complete-Arch Implant Intraoral Digital Scans." *Journal of Dentistry* 125: 104266.
- Klein, M., F. J. Tuminelli, A. Sallustio, et al. 2023. "Full-Arch Restoration With the NEXUS IOS System: A Retrospective Clinical Evaluation of 37 Restorations After a One Year of Follow-Up." *Journal of Dentistry* 139: 104741.
- Lee, H., V. Fehmer, S. Hicklin, G. Noh, S. J. Hong, and I. Sailer. 2020. "Three-Dimensional Evaluation of Peri-Implant Soft Tissue When Tapered Implants Are Placed Pilot Study With Implants Placed Immediately or Early Following Tooth Extraction." *International Journal of Oral & Maxillofacial Implants* 35: 1037–1044.
- Marchand, L., I. Sailer, H. Lee, P. Mojon, and J. Pitta. 2022. "Digital Wear Analysis of Different CAD/CAM Fabricated Monolithic Ceramic Implant-Supported Single Crowns Using Two Optical Scanners." *International Journal of Prosthodontics* 35: 357–364.
- Mizumoto, R. M., B. Yilmaz, E. A. McGlumphy, J. Seidt, and W. M. Johnston. 2020. "Accuracy of Different Digital Scanning Techniques

- and Scan Bodies for Complete-Arch Implant-Supported Prostheses." *Journal of Prosthetic Dentistry* 123: 96–104.
- Pan, Y., J. K. H. Tsoi, W. Y. H. Lam, and E. H. N. Pow. 2021. "Implant Framework Misfit: A Systematic Review on Assessment Methods and Clinical Complications." *Clinical Implant Dentistry and Related Research* 23: 244–258.
- Papaspyridakos, P., K. Chochlidakis, K. Kang, et al. 2020. "Digital Workflow for Implant Rehabilitation With Double Full-Arch Monolithic Zirconia Prostheses." *Journal of Prosthodontics* 29: 460–465.
- Papaspyridakos, P., K. Vazouras, Y. Chen, et al. 2020. "Digital vs. Conventional Implant Impressions: A Systematic Review and Meta-Analysis." *Journal of Prosthodontics* 29: 660–678.
- Pattamavilai, S., and C. Ongthiemsak. 2022. "Accuracy of Intraoral Scanners in Different Complete Arch Scan Patterns." *Journal of Prosthetic Dentistry* 131: 155–162.
- Patzelt, S. B. M., A. Emmanouilidi, S. Stampf, J. R. Strub, and W. Att. 2014. "Accuracy of Full-Arch Scans Using Intraoral Scanners." *Clinical Oral Investigations* 18: 1687–1694.
- Pozzi, A., L. Arcuri, F. Lio, A. Papa, A. Nardi, and J. Londono. 2022. "Accuracy of Complete-Arch Digital Implant Impression With or Without Scanbody Splinting: An In Vitro Study." *Journal of Dentistry* 119: 104072.
- Pozzi, A., M. Tallarico, F. Mangani, and A. Barlattani. 2013. "Different Implant Impression Techniques for Edentulous Patients Treated With CAD/CAM Complete-Arch Prostheses: A Randomized Controlled Trial Reporting Data at 3 Year Post-Loading." *European Journal of Oral Implantology* 6: 325–340.
- Retana, L., A. H. Nejat, and A. Pozzi. 2023. "Effect of Splinting Scan Bodies on Trueness of Complete-Arch Implant Impression Using Different Intraoral Scanners: An In Vitro Study." *International Journal of Computerized Dentistry* 26: 19–28.
- Revilla-León, M., D. E. Kois, and J. C. Kois. 2023a. "A Guide for Maximizing the Accuracy of Intraoral Digital Scans: Part 2—Patient Factors." *Journal of Esthetic and Restorative Dentistry* 35: 241–249.
- Revilla-León, M., D. E. Kois, and J. C. Kois. 2023b. "A Guide for Maximizing the Accuracy of Intraoral Digital Scans. Part 1: Operator Factors." *Journal of Esthetic and Restorative Dentistry* 35: 230–240.
- Revilla-León, M., M. M. Methani, and M. Özcan. 2021. "Impact of the Ambient Light Illuminance Conditions on the Shade Matching Capabilities of an Intraoral Scanner." *Journal of Esthetic and Restorative Dentistry* 33: 906–912.
- Rutkūnas, V., A. Gedrimienė, N. Al-Haj Husain, et al. 2023. "Effect of Additional Reference Objects on Accuracy of Five Intraoral Scanners in Partially and Completely Edentulous Jaws: An In Vitro Study." *Journal of Prosthetic Dentistry* 130: 111–118.
- Tasaka, A., Y. Uekubo, T. Mitsui, et al. 2019. "Applying Intraoral Scanner to Residual Ridge in Edentulous Regions: In Vitro Evaluation of Inter-Operator Validity to Confirm Trueness." *BMC Oral Health* 19: 264.
- Tohme, H., G. Lawand, M. Chmielewska, and J. Makhzoume. 2023. "Comparison Between Stereophotogrammetric, Digital, and Conventional Impression Techniques in Implant-Supported Fixed Complete Arch Prostheses: An In Vitro Study." *Journal of Prosthetic Dentistry* 129: 354–362.
- Toia, M., M. Stocchero, Y. Jinno, et al. 2019. "Effect of Misfit at Implant-Level Framework and Supporting Bone on Internal Connection Implants: Mechanical and Finite Element Analysis." *International Journal of Oral & Maxillofacial Implants* 34: 320–328.
- Wu, H. K., G. Chen, Z. Zhang, et al. 2024. "Effect of Artificial Landmarks of the Prefabricated Auxiliary Devices Located at Different Arch Positions on the Accuracy of Complete-Arch Edentulous Digital Implant Scanning: An In-Vitro Study." *Journal of Dentistry* 140: 104802.
- Wu, H. K., J. Wang, G. Chen, X. Huang, F. Deng, and Y. Li. 2023. "Effect of Novel Prefabricated Auxiliary Devices Attaching to Scan Bodies on the Accuracy of Intraoral Scanning of Complete-Arch With Multiple Implants: An In-Vitro Study." *Journal of Dentistry* 138: 104702.
- Wulfman, C., A. Naveau, and C. Rignon-Bret. 2020. "Digital Scanning for Complete-Arch Implant-Supported Restorations: A Systematic Review." *Journal of Prosthetic Dentistry* 124: 161–167.
- Zhang, T., B. Yang, R. Ge, C. Zhang, H. Zhang, and Y. Wang. 2024. "Effect of a Novel 'Scan Body' on the In Vitro Scanning Accuracy of Full-Arch Implant Impressions." *International Dental Journal* 74: 847–854.